Stability of stationary states in the cubic nonlinear Schrödinger equation: Applications to the Bose-Einstein condensate

L. D. Carr,[1,*] J. N. Kutz,[2] and W. P. Reinhardt[1,3]
[1]*Department of Physics, University of Washington, Seattle, Washington 98195-1560*
[2]*Department of Applied Mathematics, University of Washington, Seattle, Washington 98195-2420*
[3]*Department of Chemistry, University of Washington, Seattle, Washington 98195-1700*
(Received 6 July 2000; revised manuscript 11 December 2000; published 18 May 2001)

The cubic nonlinear Schrödinger equation is the quasi-one-dimensional limit of the mean-field theory which models dilute gas Bose-Einstein condensates. Stationary solutions of this equation can be characterized as soliton trains. It is demonstrated that for repulsive nonlinearity a soliton train is stable to initial stochastic perturbation, while for attractive nonlinearity its behavior depends on the spacing between individual solitons in the train. Toroidal and harmonic confinement, both of experimental interest for Bose-Einstein condensates, are considered.

DOI: 10.1103/PhysRevE.63.066604 PACS number(s): 05.30.Jp, 03.75.Fi, 05.45.Yv

I. INTRODUCTION

The one-dimensional nonlinear Schrödinger equation (NLS) is ubiquitious. Among other natural phenomena, it models dilute-gas Bose-Einstein condensates (BEC's) in the quasi-one-dimensional regime [1], light pulses in optical fibers [2], Bose-condensed photons [3], helical excitations of a vortex line [4], and spin waves in magnetic materials [5]. In this paper application of the NLS to the BEC is emphasized. As current [6–9] and proposed [10–14] BEC's are studied in traps of differing topologies, issues of stability for periodic solutions on a ring and for confinement in a harmonic potential are both of interest.

In a recent pair of articles [15,16] the full set of periodic solutions of the stationary NLS on a ring was presented in closed analytic form. It was shown that these states can be characterized as soliton trains. This paper is extended by numerically studying the stability of such stationary states in response to stochastic perturbation of the initial condition. It is demonstrated that for repulsive nonlinearity a soliton train is stable, while for attractive nonlinearity its behavior depends on the spacing between individual solitons in the train. It is argued that these stability properties may be explained in terms of the stability of single solitons [17,18] and the dynamics of soliton-soliton interactions [19–22].

The one-dimensional cubic NLS, to which these soliton trains form the full set of stationary states, is the quasi-one-dimensional limit of the three-dimensional mean-field theory that describes the dynamics of a dilute BEC at low temperature [23–25]. The *quasi-one-dimensional* (quasi-1D) regime holds when the transverse dimensions of the condensate are on the order of its healing length and its longitudinal dimension is much longer than its transverse ones [15]. If the transverse dimensions of the condensate are much less than the healing length then the three-dimensional mean-field theory no longer applies and other physical models are required [26].

For repulsive nonlinearity, soliton train stationary states have direct application in current BEC experiments. Soliton-like structures have been created and observed in three dimensions [27,28]. The trapping of a BEC in a hollow blue-detuned laser beam demonstrates that quasi-one-dimensional BEC's can be created [6] and a method for engineering standing dark solitons has recently been proposed [29]. A combination of these techniques could be used to create soliton trains. A key point in making solitons in the quasi-1D regime directly observable is the use of a boxlike, rather than harmonic, transverse confining potential, as explained in detail in Ref. [29]. The potentially quasi-1D experiment of Ref. [6] has this capacity. Alternate definitions of the quasi-1D regime, specific to harmonic transverse confinement, have been advanced [30]. We do not consider those here.

The extent to which quantum fluctuations affect the BEC remains an outstanding theoretical question [31]. Mean-field theory has so far proven to be an excellent model [7,25]. However, the extent to which the actual BEC will support highly excited states of the mean field is unknown. In this sense quantum fluctuations may already be observable in terms of their effects upon soliton trains. Recent developments [32,6] will further permit experimentalists to go beyond the approximations of diluteness, low temperature, and dimensionality inherent in the mean-field model. Soliton trains could prove useful in studying all these important aspects of the BEC.

For attractive nonlinearity, BEC's have only been experimentally studied in three-dimensional traps. Although in three dimensions the attractive BEC collapses [33–36], in quasi-1D it is predicted to be stable [1], and a number of authors have explored stablization schemes based on dimensionality and initial states [37,38]. The results presented herein suggest the optimal density and phase profiles to obtain a stable, quasi-1D attractive BEC. These criteria are equally applicable to wave phenomena in many physical situations, as for example ring lasers [39].

This paper is outlined as follows. In Sec. II the full set of periodic solutions of the stationary NLS are reviewed. In Sec. III the stability of these solutions to initial stochastic perturbation is studied numerically for both repulsive and

*Author to whom correspondence should be addressed.

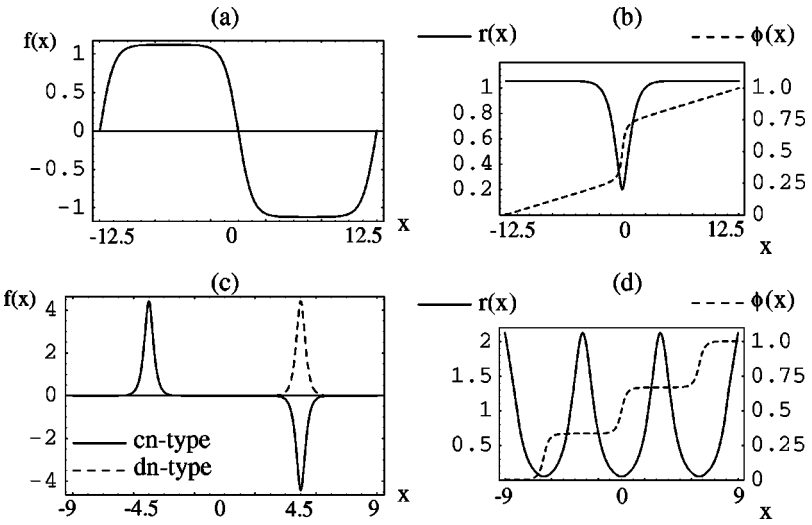

FIG. 1. Shown are the five periodic stationary solution-types in one dimension. (a) Amplitude of real solution and (b) amplitude and phase of intrinsically complex solution for repulsive nonlinearity; (c) amplitude of *dn*-type and *cn*-type solutions and (d) amplitude and phase of intrinsically complex solution for attractive nonlinearity.

attractive nonlinearity. In Sec. IV the studies are extended to the case of harmonic confinement and the solitonlike nature of the stationary states is exhibited. Finally in Sec. V the conclusions are presented.

II. PERIODIC SOLUTIONS ON THE RING

The NLS in 1D has a number of special properties that are described in the mathematical literature. It is integrable [36,40], may be solved exactly by the inverse scattering transform [19,20], and has a countably infinite number of conserved quantities [41,42]. We have taken advantage of its special properties in finding its stationary solutions. The full set of periodic stationary states of the 1D NLS on a ring of circumference L is reviewed [15,16].

Unlike in the case of the NLS on the infinite line, the finite domain considered here requires the use of an additional parameter, though integrability is retained. The cubic NLS with an additional scaling factor, which incorporates the strength of the nonlinearity, may be written

$$[-\partial_x^2 \pm \eta |f(x,t)|^2] f(x,t) = \imath \partial_t f(x,t) \tag{1a}$$

or

$$[-\xi^2 \partial_x^2 \pm |f(x,t)|^2] f(x,t) = \imath \partial_t f(x,t). \tag{1b}$$

The two forms of Eq. (1) have different physical emphases. In the first, η is proportional to the number of condensed atoms N and the s-wave scattering length between atoms; in the second, ξ is the healing length [25], which gives the length scale of variations in the condensate wave function $f(x,t)$. As $\eta \propto \xi^{-2}$, the two forms are equivalent. The $\pm$ refers to repulsive or attractive two-body atomic interactions, respectively, and x and t are rescaled space and time.

Assuming the wave function to be of the form $f(x,t) = f(x)e^{-\imath \mu t}$ results in the stationary NLS:

$$[-\partial_x^2 \pm \eta |f(x)|^2] f(x) = \mu f(x), \tag{2}$$

where μ is the eigenvalue that corresponds to the chemical potential of the BEC. All stationary solutions to Eq. (2) may be written in terms of Jacobian elliptic functions [43]. The properties of such functions are reviewed elsewhere [15,43,44]. There are five normalizable, symmetry-breaking, periodic solution-types to the stationary NLS on the ring. They are pictured in Fig. 1. All five solution types are found by solving Eq. (2) subject to normalization and boundary conditions, and are described in detail in Refs. [15] and [16].

Real stationary states in one-to-one correspondence with those of the particle-on-a-ring problem in linear quantum mechanics are

$$f(x) = A \mathrm{sn}\left[\frac{2jK(m)x}{L} + \delta \middle| m \right] \tag{3}$$

and

$$f(x) = A \mathrm{cn}\left[\frac{2jK(m)x}{L} + \delta \middle| m \right] \tag{4}$$

for repulsive and attractive nonlinearity, respectively. They shall be designated *sn-type* and *cn-type*, in accord with their functional form. For the case where $j=2$, Eq. (3) is shown in Fig. 1(a) and Eq. (4) in Fig. 1(c). A is the amplitude $j \in \{2,4,6,\ldots\}$ is the number of nodes, $K(m)$ is the complete Jacobian elliptic integral, which is the quarter period of these functions, δ is an arbitrary translational offset, which leads to a Kosterlitz-Thouless-type entropy in one dimension [45], L is the circumference of the ring, and $0 \leqslant m \leqslant 1$ is the Jacobian elliptic parameter. The general notation $\mathrm{sn}(u|m)$ is standard for Jacobian elliptic functions [43,44].

The Jacobian elliptic parameter m governs the strength of the nonlinearity η. As $m \to 0^+$, $\eta \ll 1$, sn$\to$sin, and cn $\to$cos, respectively. This is the linear, sinusoidal limit, which reproduces the particle-on-a-ring stationary solutions from linear quantum mechanics. As $m \to 1^-$, $\eta \gg 1$, sn$\to$ tanh, and cn $\to$sech. These are the dark and bright soliton, stationary solutions to the NLS on the infinite line, respectively [19,20]. This shows the connection between these stationary solutions and solitons. On the ring the jth stationary state is a $2j$ soliton train.

In addition to the above two solution types there are three nodeless, symmetry-breaking solution types that have no analog in the particle-on-a-ring problem in linear quantum mechanics. The first, a solution for attractive nonlinearity, is real

$$f(x)=A\,\mathrm{dn}\left[\frac{2jK(m)x}{L}+\delta\middle|m\right], \tag{5}$$

where $j\in\{1,2,3,\ldots\}$. It shall be designated *dn-type*. An example is shown in Fig. 1(c). The other two types are intrinsically complex. $f(x)\equiv r(x)\exp[\imath\phi(x)]$ and for repulsive nonlinearity

$$r(x)^2=A^2\left\{1-\gamma\,\mathrm{dn}^2\left[\frac{2jK(m)x}{L}+\delta\middle|m\right]\right\} \tag{6}$$

while for attractive nonlinearity

$$r(x)^2=A^2\left\{\mathrm{dn}^2\left[\frac{2jK(m)x}{L}+\delta\middle|m\right]-\gamma(1-m)\right\}, \tag{7}$$

where in both cases the phase must be found by numerical integration from the equation

$$\phi'(x)=\frac{\alpha}{r(x)^2}. \tag{8}$$

The phase and amplitude for $j=1$ and $j=3$ are shown in Figs. 1(b) and 1(d). In the repulsive case $A^2\gamma$ is the depth of the density minima below the constant background. When $\gamma=1$, Eq. (3) is recovered. In the attractive case γ interpolates between the cn-type and dn-type solutions in Eqs. (4) and (5). In both cases $0\leqslant\gamma\leqslant1$, α is a constant of integration, $j\in\{1,2,3,\ldots\}$ is the number of density minima or maxima, respectively, and each stationary state has a complex-conjugate, degenerate partner.

The intrinsically complex solutions for repulsive nonlinearity are interpreted as density-notch solitons moving with speed c on the ring with an opposing momentum boost of the condensate of speed $-c$, which results in a stationary state in the lab frame. Density-notch solitons have a speed between zero and the Boguliubov sound speed, ranging from maximal to zero depth, respectively [46]. Those not of maximal depth are called gray solitons, while those that are of maximal depth and therefore form a node are called dark solitons. Figure 1(b) shows the bounded, quantized version of a stationary gray soliton on a ring.

All attractive symmetry-breaking, longitudinally periodic, stationary solution types, i.e., the cn and dn types shown in Fig. 1(b) and the intrinsically complex one shown in Fig. 1(d), are described by the C_j point symmetry group, where j is the number of peaks. There are j nearly degenerate solutions. For even j there is a real dn-type-cn-type pair and $(j-2)/2$ degenerate intrinsically complex pairs. For odd j there is a real dn-type solution and $(j-1)/2$ degenerate intrinsically complex pairs. Thus by group theory these three solution types form the complete set of periodic stationary states made of evenly spaced peaks.

The existence of nodeless solutions requires a minimum η [15,16]. Based on this bound, the effective interaction length of a soliton is $2\pi\sqrt{6}\xi$ or $2\pi\sqrt{2}\xi$ for repulsive or attractive nonlinearity. In our plots we shall choose $\xi=1$ and let the length of the ring determine the strength of the nonlinearity, since on a finite interval the important quantity is ξ/L. Three scale regimes are then defined as follows: $j\xi/L\ll1$ is the *well-separated* regime, $j\xi/L\sim1$ is the *adjacent* regime, and $j\xi/L\gg1$ is the *overlapping* regime. These three regimes are especially important for attractive nonlinearity, as shall be seen in Sec. III B.

III. DYNAMICS UNDER INITIAL STOCHASTIC PERTURBATION

Recent theoretical studies of soliton stability with application to the BEC have focused on a single dark soliton in unbounded or harmonic confinement [30,47,48]. These studies have considered the Boguliubov-de Gennes method of linearizing [49] around solutions of the NLS and have predicted that a single dark soliton accelerates in a diffusive manner, similiar to Gordon-Haus jitter [51], essentially by reflecting phonons, which are a limit of Bogoliubov quasiparticle excitations. Ruprecht *et al.* [50] showed that Boguliubov excitations correspond to the resonances of the linear response of the wave function when the NLS is driven harmonically. In the same article it was shown that the *nonlinear* response is also very important, as for example in the creation of large amplitude harmonics.

Our approach is to consider the full response, i.e., both linear and nonlinear, of soliton train stationary states to initial stochastic perturbation. The cases of both repulsive and attractive nonlinearity are treated. This forms a reference for stability studies and, in the repulsive case, answers the question of whether soliton trains could be experimentally created as an initial state and whether they persist within the context of the NLS. Stochastic noise could represent any imperfection in the creation process, as for example, in the trapping potential. It has the further advantage of matching the extensive stability studies of single bright [51,17] and dark [49,18] solitons undertaken in the context of nonlinear optics. The subsequent question of whether soliton train stationary states have a lifetime associated with thermal fluctuations in the form of Boguliubov quasiparticles or higher-order quantum effects is under investigation elsewhere [52].

Specifically, our numerical investigation involves the addition of initial stochastic noise into the time evolution of the stationary states presented in Sec. II. The algorithm employed uses a fourth-order Runge-Kutta in time and a filtered pseudospectral method in space to propagate solutions over space-time intervals of interest. Stochastic noise is included by adding to every Fourier mode a Gaussian distributed random number with mean zero and unit variance multiplied by a strength coefficient. The strength coefficient utilized in the figures shown in the following sections is typically 0.5 divided by the number of Fourier modes. However, a wide range of strength coefficients was tested and the results are

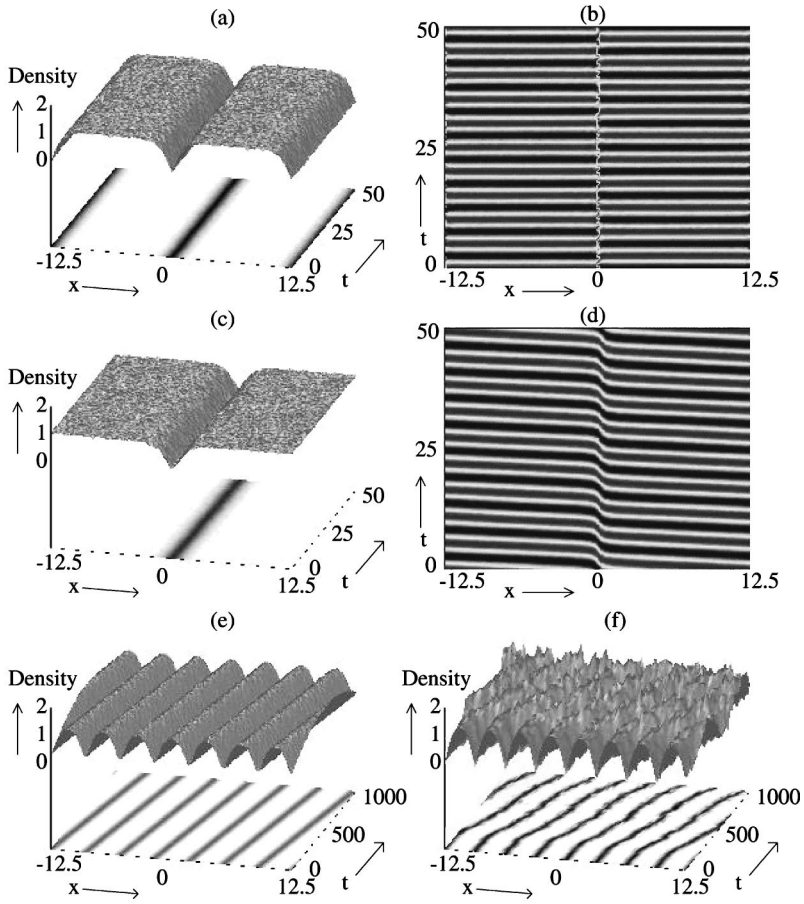

FIG. 2. Stability for repulsive nonlinearity, periodic solutions on the ring. (a) Density and (b) phase of real, sn-type solution with initial stochastic noise; (c) density and (d) phase of intrinsically complex solution. The lowest-energy solution is shown for each type. A short-time scale was used to illuminate the phase but the same stability properties hold over an order of magnitude longer time. The phase is plotted mod 2π. (e) Highly excited intrinsically complex solutions are stable to perturbation by initial stochastic noise, despite slow drift. (f) Continuous noise builds up because there is no dissipation term in the NLS, but even highly excited solutions exhibit at most a diffusive drift similiar to the Gordon-Haus jitter of a single soliton.

not dependent on the strength of the noise, provided that its amplitude is not on the same order as that of the stationary states. Although some solutions are illustrated over short-time scales for presentation purposes, all simulations were performed over time scales longer than experimental lifetimes of the BEC [1].

A. Repulsive nonlinearity

In response to stochastic noise, density-notch soliton trains drift but are otherwise stable. This may be understood by extrapolation from the stability properties of single solitons. Single density-notch solitons respond to stochastic perturbation by emission of radiation and by a change in velocity and depth. Velocity and depth are a function of a single parameter, sometimes called the soliton phase angle. A full analysis requires separate consideration of the constant background and the density notch. Kivshar and Yang [18] have completed this analysis for single solitons on the infinite line by using a variational approach.

In Figs. 2(a) and 2(b) the evolution of a sn-type stationary state described by Eq. (3) with initial stochastic noise is shown. This is the lowest such state on the ring. On a longer-time scale there is some drift. In this case the two density notches retain their spacing and phase relationship. In the box this same stationary state is the first excitation above the ground state. Numerical studies, though not shown here, reveal that the single density notch in the center drifts randomly between the box boundaries until it comes close to one, at which point it reverses direction abruptly. This can be explained by interpreting the falling off of the wave function at the boundaries as pinned solitons [46], which repel the central density notch when it comes within the interaction length of $\pi\sqrt{6}\xi$.

In Figs. 2(c) and 2(d) the evolution of an intrinsically complex stationary state described by Eqs. (6) and (8) with initial stochastic noise is shown. This is the lowest symmetry-breaking state on the ring. It consists of both a background phase ramp and a density notch, and is quite stable. Because phase quantum number is conserved for the NLS, the background cannot be perturbed into a lower-energy state. A gray density notch has the same response to perturbation as a dark density notch. Therefore the two together emit radiation and, on longer-time scales, drift, but remain otherwise unchanged.

In Fig. 2(e) the evolution of a highly excited state is shown. This demonstrates that for repulsive nonlinearity, there is no difference between the stability properties of soliton-train stationary states in the overlapping, adjacent, or well-separated regimes, a fact not *a priori* apparent from single soliton considerations. In Fig. 2(f), continuous stochastic noise is added. This perturbs the equation rather than the initial solution. As there is no dissipative term in the NLS, the noise builds up over 1000 time units to a very high level. The soliton train exhibits diffusive drift, similiar to the Gordon-Haus jitter of a single dark soliton [49]. Lastly, though not shown here, we note that the addition of quintic

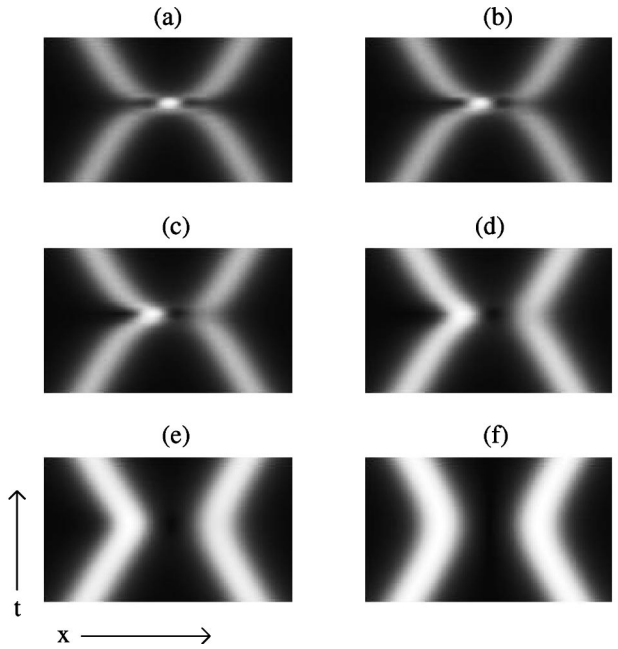

FIG. 3. Phase dependence of bright soliton interactions. Shown are the space-time projection of the density of colliding bright solitons. The phase difference between the two solitons is (a) 0, (b) $\pi/16$, (c) $\pi/8$, (d) $\pi/4$, (e) $\pi/2$, and (f) π. The time scale in each case is 50 time units and the interaction length is $2\pi\sqrt{2}$. Note that the circumference of the ring is much greater than the length scale shown here.

nonlinearity on the level of 10% has no destabilizing effect upon soliton-train stationary states.

B. Attractive nonlinearity

The study of soliton trains differs from that of single solitons or two-soliton interactions because it no longer suffices to consider the well-separated limit. The exact equation for interactions between two bright solitons has been derived in full by Gordon [22]. As it is difficult to interpret when the solitons are not well separated, he has considered the nonoverlapping limit and found

$$\ddot{q} = -4\exp(-2q)\cos(2\Psi),$$
$$\ddot{\Psi} = 4\exp(-2q)\sin(2\Psi), \tag{9}$$

where $2q$ is the separation of the two solitons and 2Ψ is their relative phase. The interaction depends exponentially on the separation and sinusoidally on the relative phase. Desem and Chu [53] used this work to evaluate interaction minimization schemes in the context of fiber optics.

We found that the key to understanding the stability of intrinsically complex stationary states perturbed by initial stochastic noise for attractive nonlinearity lay in the overlapping regime of these two soliton interactions. Figure 3 shows the results of our studies. Following the six subpanels of the figure from left to right and top to bottom, it is apparent that the topology of the space-time profile changes from connected to disconnected as the phase varies from 0 to π. A hole opens in the center, rotates, and then separates the density profiles of the two solitons. Thus the interaction changes continuously from completely attractive to completely repulsive. For $2\Psi \in [\pi, 2\pi]$ the topology reverses itself in the same way.

Single bright solitons respond to stochastic perturbation not only by emission of radiation and by a change in velocity, but also by a drift in phase [17]. As a soliton train requires a fixed phase relationship between its components, it is to be expected that the stability properties of solitons trains for attractive nonlinearity differ from those of repulsive nonlinearity, as may be seen, for example, in the numerical studies of densely packed solitons by Arbel and Orenstein [39].

In Figs. 4(a) and 4(b) the evolution of a cn-type stationary state described by Eq. (4) is shown with initial stochastic noise. In the adjacent regime this solution is quite stable out to very long-time scales. However, in the overlapping re-

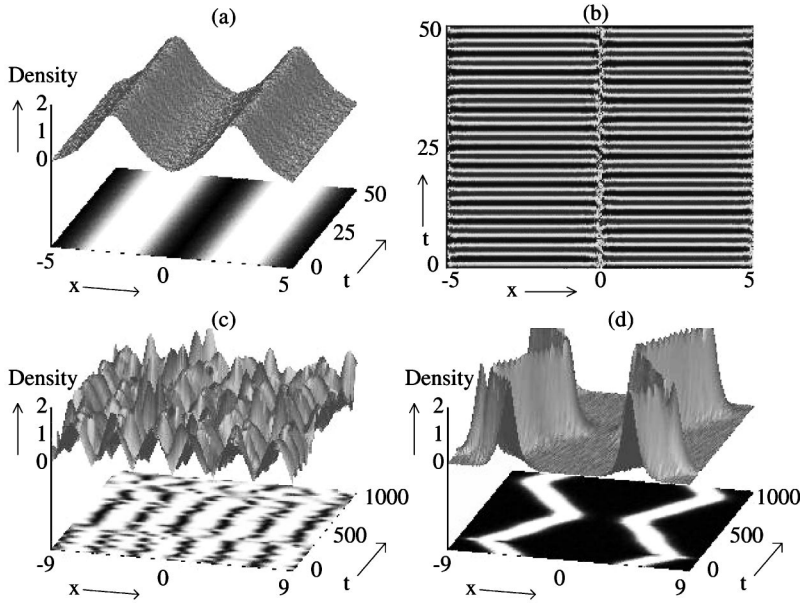

FIG. 4. Stability and the importance of scale, attractive nonlinearity. (a) Density and (b) phase of the cn-type solution with initial stochastic noise in the adjacent regime. The phase is plotted mod 2π. However, in the (c) overlapping and (d) well-separated regimes, the perturbed cn-type solution is unstable.

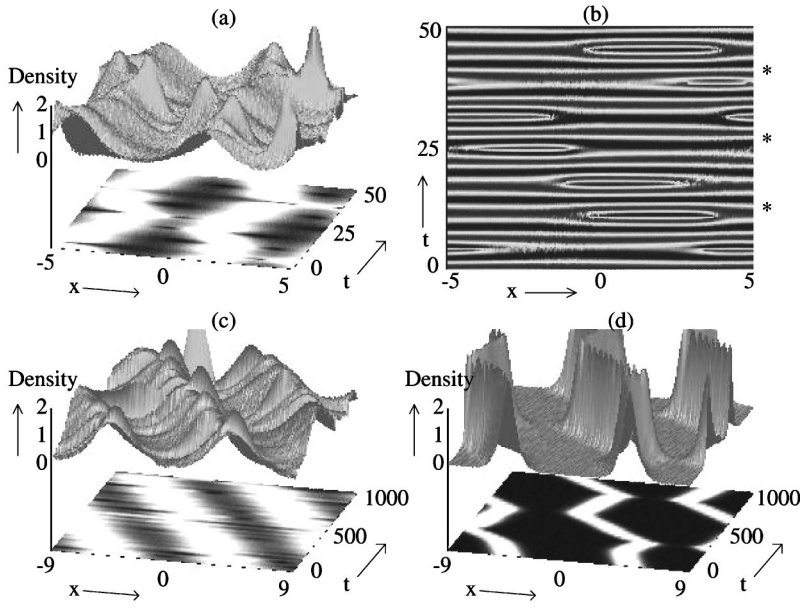

FIG. 5. Quasiperiodic stability and the importance of scale, attractive nonlinearity. (a) Density and (b) phase of the nodeless, dn-type solution with initial stochastic noise in the adjacent regime. The asterisks in (b) mark the recurrence of the solution, clearly visible here on a short-time scale. (c) On longer-time scales, but still in the adjacent regime, the peaks exchange mass and drift, but continue to recur. (d) In the well-separated regime the density peaks behave as independent solitons. Although not shown here, the perturbed dn-type solution is also unstable in the overlapping regime.

gime, such a stationary state undergoes interactions, while in the well-separated regime the peaks behave as individual solitons, as may be seen in Figs. 4(c) and 4(d). The drift in phase is especially evident in Fig. 4(d), where in the first interaction there is clearly density exhange between the two solitons, despite their initial phase difference being π.

In Figs. 5(a) and 5(b) the evolution of a real dn-type stationary state described by Eq. (5) is shown with initial stochastic noise in the adjacent regime. As the phase difference between peaks is zero, it is not surprising that the solution seems to quickly go unstable. However, there are quasiperiodic recurrences, which are noted with asterisks in Fig. 5(b). For this reason the solutions are termed *quasiperiodically* stable. This is especially evident on the longer-time scale shown in Fig. 5(c), where it may be seen that though the peaks continue to exchange mass the overall integrity of the soliton train remains intact. The drift of the train is similiar to that found for the cn-type stationary states in the adjacent regime, and as before, in the overlapping regime, it is unstable, while in the well-separated regime the peaks behave as independent solitons.

The intrinsically complex stationary states have similiar properties to the real dn-type stationary states; in the adjacent regime they evolve and retain their overall integrity, and in other regimes they are unstable. However, even in the unstable case they do not ever superimpose to make a sharp peak. This is due to the conservation of phase quantum number by the NLS. For the BEC, this is an important point. In higher dimensionality, solutions to the NLS with attractive nonlinearity collapse. This occurs when the density becomes large enough for the nonlinear term to dominate the kinetic energy. A highly excited, intrinsically complex stationary state, though unstable, can lower the maximum density by a factor of 40 or more, thereby preventing collapse.

IV. EXTENSION TO HARMONIC CONFINEMENT

Since many BEC experiments involve magneto-optical traps [7], the consideration of the stability properties of the stationary states of such a potential has immediate experimental relevance. A harmonic confining potential is added to Eq. (1b) and it is rescaled to the form

$$[-\partial_x^2 \pm \eta|f(x,t)|^2 + ax^2]f(x,t) = \imath \partial_t f(x,t), \qquad (10)$$

where a measures the strength of the harmonic trap and η the strength of the nonlinearity, which is proportional to the number of condensed atoms. As before, we consider the class of stationary solutions to Eq. (10) by letting $f(x,t) = f(x)e^{-i\mu t}$, so that

$$[-\partial_x^2 \pm \eta|f(x,t)|^2 + ax^2]f(x) = \mu f(x) \qquad (11)$$

is the resulting eigenvalue problem with eigenvalue μ.

A. Stability of stationary states

With the addition of a harmonic potential the NLS is no longer exactly integrable and closed-form solutions can no longer be obtained. However, the normalized eigenfunctions of Eq. (11) can be constructed numerically via standard shooting methods [54]. Figure 6 depicts the stationary solutions of Eq. (11) normalized to unity with $a=0.02$ and $\eta = 1$. In Figs. 6(a) and 6(b) the zeroth, first, and sixth modes are depicted for attractive and repulsive nonlinearity, respectively. In the lower modes, it is seen that attractive nonlinearity sharpens the peaks and troughs while repulsive nonlinearity makes them spread out. Highly excited states, as for example the sixth mode, are further in the linear regime, and therefore resemble the Hermite polynomial stationary solutions to the analogous problem in linear quantum mechanics. These results are qualitatively in accord with the sn-type and cn-type closed-form [15,16] stationary states for box or periodic boundary conditions.

To study the stability of these states a substantial initial stochastic-noise perturbation was added and then Eq. (10) was solved. The zeroth through sixth modes were tested, but only the first and sixth ones are illustrated. In accord with the

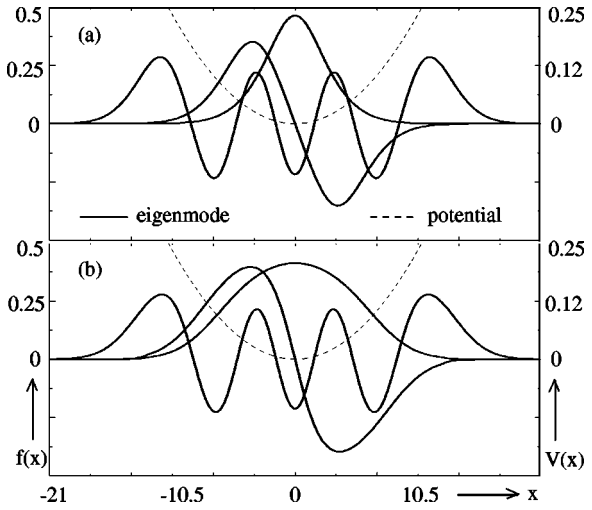

FIG. 6. Stationary states of the harmonic potential for (a) attractive and (b) repulsive nonlinearity. Pictured are the ground state, first mode, and sixth mode. Note that states in the overlapping regime, such as the sixth mode, are predominantly linear, while those in the adjacent regime, such as the first mode, are strongly nonlinear. There is no well-separated regime in the harmonic potential.

results of Sec. III it was expected that all solutions would be stable for repulsive nonlinearity, while for attractive nonlinearity they would be stable in the adjacent but not the overlapping regime. Note that here there is no well-separated regime, due to the effect of the harmonic potential.

Figures 7(a)–7(d) and 7(d) depicts the results of the simulations for $a=0.02$ and $\eta=1$ for a time of $t=1000$ for attractive and repulsive nonlinearity, respectively. Both the perturbed attractive and repulsive stationary states are observed to be stable over very long times. Figure 7(b) however, starts to exhibit an oscillatory instability at long times, much like that observed for the overlapping regime in Sec. III B.

Although not illustrated here, the effect of either negative or positive quintic nonlinearity on the order of 10% is to slightly deform the eigenstates but leave them otherwise unaffected.

B. Phase engineering

Phase engineering has been used to successfully create solitonlike structures in BEC's confined in a harmonic potential [28,27]. Specifically, a step function in the phase is used to create a density notch, which then propagates across the condensate. It has been shown elsewhere [1,46] that in quasi-one-dimensional confinement, both bright and dark solitons may be manipulated, or phase engineered, by various simple phase profiles. Here it is shown that the same is true of excited states in a harmonic potential.

To induce dynamics in the stationary states, the eigenfunction solutions depicted in Fig. 6 were modified by introducing the following two phase profiles into the initial conditions:

$$\text{I:} \quad f(x,0)=f(x)\exp(i\beta x), \tag{12}$$

$$\text{II:} \quad f(x,0)=f(x)\exp(i\beta|x|), \tag{13}$$

where β determines the phase perturbation strength. For profile I, all peaks are ramped in the same fashion, whereas for profile II, the peaks are ramped in opposite directions initially depending upon their location in x.

Figure 8 illustrates the resulting dynamics for both attractive and repulsive nonlinearity. In Figs. 8(a) and 8(c), phase profile II is imposed on the first mode for $a=0.02$, $\eta=1$, and $\beta=0.3$. This initially leads to a repulsion of the peaks. However, the potential counteracts this effect and the peaks undergo an oscillatory particlelike motion. In contrast, phase profile I keeps the peaks moving in unison and the potential once again acts to trap the peaks inside the potential by generating a periodic motion within the well. These two cases are analogous to the oscillatory eigenmodes of the coupled pendulum, and clearly demonstrates the solitonlike behavior of the stationary states when phase engineered. Thus in the

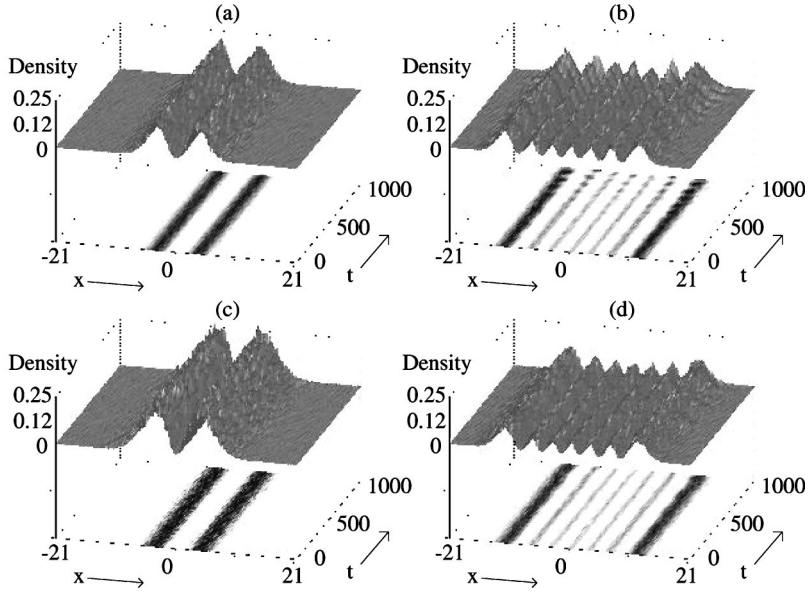

FIG. 7. Stability of stationary states in the harmonic potential. The first and sixth modes are propagated with initial stochastic noise over long-time scales for (a) and (b) attractive nonlinearity and (c) and (d) repulsive nonlinearity. The stability properties are identical to those of the analogous solutions for periodic solutions on the ring: only (b) shows instability, as it is for attractive nonlinearity in the overlapping regime.

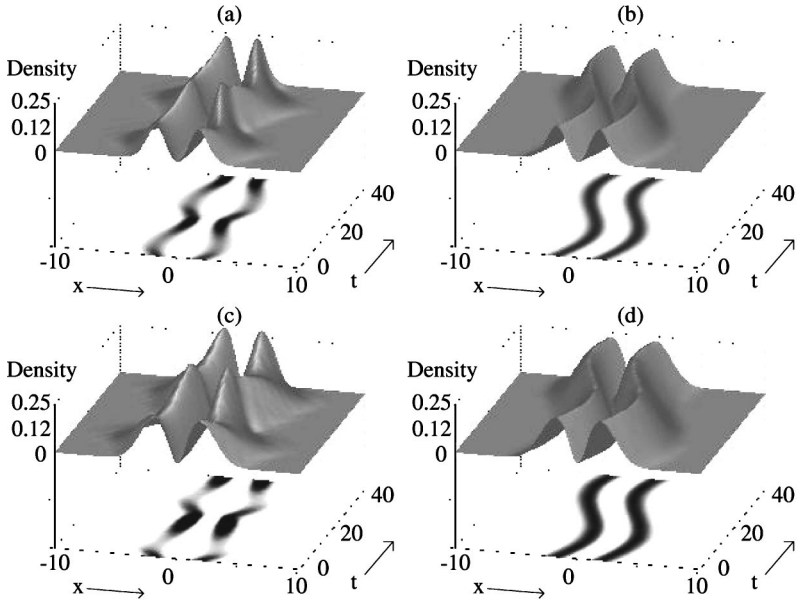

FIG. 8. Phase engineering of stationary states in the harmonic potential. The particlelike nature of these solutions is exhibited for both (a) and (b) attractive nonlinearity and (c) and (d) repulsive nonlinearity. In (a) and (c) an equal and opposite linear phase ramp was used on the two density peaks, while in (b) and (d) an identical phase ramp was used. This produces two oscillatory modes analogous to those of the coupled pendulum.

mean-field approximation the BEC, itself consisting of particles, has solutions of a particlelike nature.

V. CONCLUSION

The essential stability results of single bright and dark solitons perturbed by initial stochastic noise have been extended to soliton trains. For repulsive nonlinearity a soliton train responds as a unit, while for attractive nonlinearity, its behavior depends on how tightly packed the individual solitons in the train are. As the NLS models trapped dilute gas Bose-Einstein condensates, and the full set of periodic solutions to the stationary NLS can be characterized as soliton trains, these studies apply to the BEC.

In particular, the stability results presented here show that if excited stationary states of the BEC can be created via developing experimental techniques [28,27,6], instabilities beyond the usual diffusive drift known as Gordon-Haus jitter [51,49] would be indicative of higher-order quantum effects. Our results also give a prescription for keeping the density of an attractive BEC low and thereby preventing collapse; density peaks of alternating phase should be engineered in the adjacent regime, i.e., they should neither overlap strongly nor be sufficiently well-separated so as to behave as independent solitons.

Finally, it was shown that stationary states of the NLS with a harmonic potential, which is especially relevant to current BEC experiments, had similiar stability properties to the case of periodic solutions on the ring treated above. The solitonlike nature of such stationary states was illustrated.

ACKNOWLEDGMENTS

The authors benefited greatly from discussions with David Thouless and Mary Ann Leung. Sarah McKinney and Joachim Brand provided additional computational assistance. This work was supported by the National Science Foundation Grant No. CHE97-32919 for L. D. Carr and W. P. Reinhardt and Grant No. DMS-9802920 for J. N. Kutz.

[1] L. D. Carr, M. A. Leung, and W. P. Reinhardt, J. Phys. B **33**, 3983 (2000).
[2] A. Hasegawa, *Optical Solitons in Fibers* (Springer-Verlag, New York, 1990).
[3] R. Y. Ciao, I. H. Deutsch, J. C. Garrison, and E. W. Wright, *Frontiers in Nonlinear Optics: the Serge Akhmanov Memorial Volume* (Institute of Physics, Bristol, 1993), p. 151.
[4] H. Hasimoto, J. Fluid Mech. **51**, 477 (1972).
[5] B. A. Kalinikos, M. M. Scott, and C. E. Patton, Phys. Rev. Lett. **84**, 4697 (2000).
[6] K. Bongs *et al.*, e-print cond-mat/0007381.
[7] W. Ketterle, D. S. Sturfee, and D. M. Stamper-Kurn, in *Proceedings of the International School of Physics ''Enrico Fermi''* (IOS, Amsterdam, 1999), pp. 67–176.
[8] M. R. Matthews *et al.*, Phys. Rev. Lett. **83**, 2498 (1999).
[9] J. E. Williams and M. J. Holland, Nature (London) **401**, 568 (1999).
[10] E. M. Wright, J. Arlt, and K. Dholakia, Phys. Rev. A **63**, 013608 (2001); e-print cond-mat/0008479.
[11] J. D. Close and W. Zhang, J. Opt. B: Quantum Semiclassic. Opt. **1**, 420 (1999).
[12] J.-P. Martikainen, K.-A. Suominen, and A. Sanpera, e-print cond-mat/0005136.
[13] M. Key *et al.*, Phys. Rev. Lett. **84**, 1371 (2000).
[14] N. H. Dekker *et al.*, Phys. Rev. Lett. **84**, 1124 (2000).
[15] L. D. Carr, C. W. Clark, and W. P. Reinhardt, Phys. Rev. A **62**, 063610 (2000).
[16] L. D. Carr, C. W. Clark, and W. P. Reinhardt, Phys. Rev. A **62**, 063611 (2000).
[17] J. N. Elgin, Phys. Rev. A **47**, 4331 (1993).

[18] Y. S. Kivshar and X. Yang, Phys. Rev. E **49**, 1657 (1994).
[19] V. E. Zakharov and A. B. Shabat, Zh. Éksp. Teor. Fiz. **61**, 118 (1971) [Sov. Phys. JETP **34**, 62 (1971)].
[20] V. E. Zakharov and A. B. Shabat, Zh. Éksp. Teor. Fiz. **64**, 1627 (1973) [Sov. Phys. JETP **37**, 823 (1973)].
[21] L. Lerner, D. J. Mitchell, and A. W. Snyder, Opt. Lett. **19**, 1302 (1994).
[22] J. P. Gordon, Opt. Lett. **8**, 596 (1983).
[23] E. P. Gross, Nuovo Cimento **20**, 454 (1961).
[24] L. P. Pitaevskii, Zh. Éksp. Teor. Fiz. **40**, 646 (1961) [Sov. Phys. JETP **13**, 451 (1961)].
[25] F. Dalfovo, S. Giorgini, L. P. Pitaevskii, and S. Stringari, Rev. Mod. Phys. **71**, 463 (1999).
[26] D. S. Petrov, G. V. Shylapnikov, and J. T. M. Walraven, Phys. Rev. Lett. **85**, 3745 (2000).
[27] S. Burger *et al.*, Phys. Rev. Lett. **83**, 5198 (1999).
[28] J. Denschlag *et al.*, Science **287**, 97 (2000).
[29] L. D. Carr, S. Burger, and A. Sanpera, Phys. Rev. A (to be published), e-print cond-mat/0011397.
[30] A. E. Muryshev, H. B. van Linden van den Heuvell, and G. V. Shlyapnikov, Phys. Rev. A **60**, R2665 (1999).
[31] S. A. Morgan, J. Phys. B **33**, 3847 (2000).
[32] S. L. Cornish *et al.*, Phys. Rev. Lett. **85**, 1795 (2000); e-print cond-mat/0004290.
[33] C. C. Bradley, C. A. Sackett, J. J. Tollett, and R. G. Hulet, Phys. Rev. Lett. **75**, 1687 (1995).
[34] C. C. Bradley, C. A. Sackett, and R. G. Hulet, Phys. Rev. A **55**, 3951 (1997).
[35] C. A. Sackett, J. M. Gerton, M. Welling, and R. G. Hulet, Phys. Rev. Lett. **82**, 876 (1999).
[36] C. Sulem and P. L. Sulem, *Nonlinear Schrödinger Equations: Self-focusing Instability and Wave Collapse* (Springer-Verlag, New York, 1999).
[37] H. Michinel, V. M. Pérez-García, and R. de la Fuente, Phys. Rev. A **60**, 1513 (1999).
[38] L. Berge, T. J. Alexander, and Y. S. Kivshar, Phys. Rev. A **62**, 023607 (2000); e-print cond-mat/9907408.
[39] D. Arbel and M. Orenstein, IEEE J. Quantum Electron. **35**, 977 (1999).
[40] Y. S. Kivshar, Phys. Rep. **298**, 81 (1998).
[41] R. M. Miura, J. Math. Phys. **9**, 1202 (1968).
[42] R. M. Miura, S. C. Gardner, and M. D. Kruskal, J. Math. Phys. **9**, 1204 (1968).
[43] F. Bowman, *Introduction to Elliptic Functions, with Applications* (Dover, New York, 1961).
[44] *Handbook of Mathematical Functions*, edited by M. Abramowitz and I. A. Stegun (National Bureau of Standards, Washington, D. C., 1964).
[45] J. M. Kosterlitz and D. J. Thouless, J. Phys. C **6**, 1181 (1973).
[46] W. P. Reinhardt and C. W. Clark, J. Phys. B **30**, L785 (1997).
[47] P. O. Fedichev, A. E. Muryshev, and G. V. Shlyapnikov, Phys. Rev. A **60**, 3220 (1999).
[48] T. Busch and J. R. Anglin, Phys. Rev. Lett. **84**, 2298 (2000).
[49] Y. S. Kivshar, M. Haelterman, P. Emplit, and J.-P. Hamaide, Opt. Lett. **19**, 19 (1994).
[50] P. A. Ruprecht, M. Edwards, K. Burnett, and C. W. Clark, Phys. Rev. A **54**, 4178 (1996).
[51] J. P. Gordon and H. A. Haus, Opt. Lett. **11**, 665 (1986).
[52] S. A. Morgan, University of Oxford (private communication).
[53] C. Desem and P. L. Chu, IEE Proc. J. **134**, 145 (1987).
[54] Y. S. Kivshar, T. J. Alexander, and S. K. Turitsyn, Phys. Rev. Lett. (to be published), e-print cond-mat/9907475.